



OpenAIR@RGU

The Open Access Institutional Repository at Robert Gordon University

<http://openair.rgu.ac.uk>

This is an author produced version of a paper published in

IOP Conference Series: Materials Science and Engineering (ISSN 1757-8981, eISSN 1757-899X)

This version may not include final proof corrections and does not include published layout or pagination.

Citation Details

Citation for the version of the work held in 'OpenAIR@RGU':

ANSARI, F., SACHSE, S., MICHALOWSKI, S., KAVOSH, M., PIELICHOWSKI, K. and NJUGUNA, J., 2014. Characterization of synthesized polyurethane/montmorillonite nanocomposite foams. Available from *OpenAIR@RGU*. [online]. Available from: <http://openair.rgu.ac.uk>

Citation for the publisher's version:

ANSARI, F., SACHSE, S., MICHALOWSKI, S., KAVOSH, M., PIELICHOWSKI, K. and NJUGUNA, J., 2014. Characterization of synthesized polyurethane/montmorillonite nanocomposite foams. IOP Conference Series: Materials Science and Engineering, 64, pp. 012039



This work is licensed under a
[Creative Commons Attribution 3.0 Unported License.](https://creativecommons.org/licenses/by/3.0/)

Copyright

Items in 'OpenAIR@RGU', Robert Gordon University Open Access Institutional Repository, are protected by copyright and intellectual property law. If you believe that any material held in 'OpenAIR@RGU' infringes copyright, please contact openair-help@rgu.ac.uk with details. The item will be removed from the repository while the claim is investigated.

Characterization of synthesized polyurethane/montmorillonite nanocomposites foams

Farahnaz Ansari¹, Sophia Sachse², S. Michalowski³, Masoud Kavosh²
Krzysztof Pieliowski³ and James Njuguna^{*1}

¹ Innovation, Design and Sustainability, School of Engineering, Robert Gordon University, Aberdeen, AB10 7GJ, UK

² Cranfield University, Bedfordshire, MK43 0AL, UK

³ Department of Chemistry and Technology of Polymers, Cracow University of Technology, ul. Warszawska 24, 31-155 Kraków, Poland

* Correspondance aurther E-mail: j.njuguna@rgu.ac.uk

Abstract. Nanophased hybrid composites based on polyurethane/montmorillonite (PU/MMT) have been fabricated. The nanocomposite which was formed by the addition of a polyol premix with 4,4'-diphenylmethane diisocyanate to obtain nanophased polyurethane foams which were then used for fabrication of nanocomposite panels has been shown to have raised strength, stiffness and thermal insulation properties. The nanophased polyurethane foam was characterized by means of scanning electron microscope (SEM), transmission electron microscope (TEM) measurements and X-ray diffraction (XRD). TEM and SEM analysis indicated that nanophased particles are dispersed homogeneously in the polyurethane matrix on the nanometer scale indicating that PU/MMT is an intercalated nanocomposite with a 2-3 nm nanolayer thickness.

1. Introduction

In the last 20 years, there has been a strong interest in the development of polymeric nanocomposites. Nanocomposite has been successfully produced with many polymers including polyamide, polystyrene, polycaprolactone, poly (methyl methacrylate), and epoxy resin and others [1–9]. The most versatile class of polymers is polyurethane (PU) due to its excellent physical properties, e.g. flexibility at low temperature, abrasion resistance, variable hardness, etc. However, PU has the drawbacks of low thermal stability and mechanical strength. A focus of recent efforts to improve its properties has been the addition of inorganic filler (including nanoclays) in order to increase the properties of the polymer matrix [10, 11]. With improvements in the mechanical, thermal, and gas barrier properties of the polymers [12-16], PU nanocomposites are attractive for various applications from aerospace components, automobiles, ships, ballistic vests, sporting goods and helmets through to providing heat shielding, structural stiffness and crash energy management for racing cars, among several others applications.

In general there are two properties of nanocomposites that are distinctly different from other materials: i) large surface area for a given volume and ii) quantum effects [17]. Since many important chemical and physical interactions are governed by surface properties [18, 19], a nanostructured material can have substantially different properties from a bulk scale material of the same



composition. Therefore this area requires fundamental studies of mechanical, electrical, thermal, optical, and chemical properties along with related research for real applications.

For the variety of practical applications we synthesized PU/MMT and developed nanocomposite preparations [20]. As a preliminary to these, this study presents the characterization of the morphology of PU/MMT and the dispersion of nanoparticles by SEM and TEM. The structural and morphological data will be used to prepare well-defined lab materials with known composition that correspond to the currently used industrial materials.

2. Synthesis of nanophased foam

Material and preparation of nanocomposites Polyurethane foam with different weight percentages (up to 10%) of nanoclay was manufactured in four steps at the Department of Chemistry and Technology of Polymers (Cracow University of Technology, Poland). Polyol blend (polyether RF-551) and polyester (T-425R) mixture from Alfasystems, Brzeg Dolny, Poland, was stirred with powdered MMT (Optibent 987, Süd Chemie AG, Moosburg, Germany). Catalyst (N,N-dimethyl cyclohexylamine) water and surfactant (SR-321, Union Carbide, Marietta, GA) were added in order to prepare the polyol premix (component A). N-pentane as a physical blowing agent was added to component A. Component B was polymeric 4,4'-diphenylmethane diisocyanate (PM 200). It was added to component A and the mixture was stirred for 10 seconds with an overhead stirrer. Prepared mixtures were dropped into a mould. All the experiments were performed at ambient temperature of ca. 20 °C.

3. Characterization

3.1. X-ray diffraction

The Powder X-ray diffraction (XRD) θ - 2θ studies were performed with scattering angle, θ ranging between 0° and 90° using nickel-filtered Cu K α ($\lambda = 0.154$ nm) radiation at a scan rate of 1°/min. The XRD pattern of the PU/MMT indicates the presence of predominantly montmorillonite Na-Mg-Al-Si4O11 crystals.

3.2. Scanning electron microscopy (SEM) analysis

The morphology of the samples was investigated by using a FEI XL30 field emission scanning electron microscope. The operating voltage was in the range of 10–20 kV to minimize charging of the sample. The SEM images were not subjected to quantitative analysis, but merely served to gain a visual impression and it uses the reflection properties of surfaces for imaging it should be possible to visualize the binding of nanoparticles on the surface. In this attempt the fracture surface of nanocomposites were sputter coated with gold before observation.

3.3. Transmission electron microscopy (TEM) analysis

A JEOL-200CX transmission electron microscope was used to investigate the morphology of sample. For TEM studies samples were first washed by placing the nanocomposite into ultrapure water and sonicating for 2 hours. After centrifugation (6000g for 10 min), the final separated slurry was sonicated for approximately 5 min to better disperse the nanoparticles. A drop was placed on a carbon-coated copper TEM grid (200–300 mesh) and then left to dry in air.

3.4. Morphology Structure

Low impact tests were conducted using an instrumented falling weight impact device (drop tower). The device was equipped with data acquisition system to acquire force versus time data. Impact energy and velocity can be set as control factor by changing the mass and height of the dropping weight. The velocity of the falling striker is measured just before the striker hits the specimen. The specimen is held in place by fixture at the bottom of the drop tower. The impact test was performed by placing PU/MMT samples (H 50mm, W 35mm, D 25mm) bottom of the drop tower and fixed by two beams.

4. Results and discussion

4.1. XRD

XRD analysis was performed in order to understand the chemical composition of the clay. Peaks identified on the θ - 2θ scans were compared to those stored in the Joint Committee on Powder Diffraction Standards (JCPDS) database allowing identification of both crystal structure and specific crystal planes (Fig. 1).

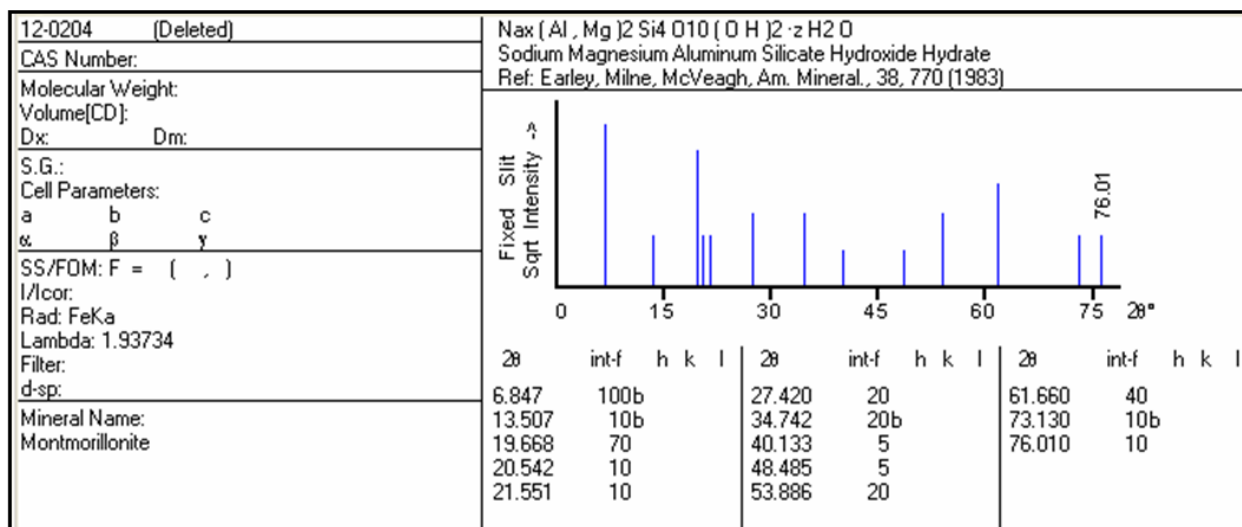


Figure 1. XRD pattern of Montmorillonite (Clay), Na_x(Al,Mg)₂Si₄O₁₀(OH)₂·zH₂O.

The XRD curves of the PU/MMT are presented in Fig. 2. The discernible peaks which can be clearly identified in the scan in Fig. 2 can be matched to, the (6.9), (13.5), (19.7), (21.5), (27.0), (35.0), (48.5), (54.0), (61.76), (73.13), and (76.68) planes of a cubic MMT unit cell.

4.2. SEM

Fig. 3 shows a SEM microphotograph of the clay/polyurethane nanocomposite. The nanolayers (observed as small spots) were approximately 3-5 nm thick and well dispersed on the surface of the polyurethane. Although not indicated in the microphotographs the clay was distributed in the deep-dark region (the cavity of the polyurethane foam structure). The SEM results indicate that the MMT particles are completely disordered and dispersed relatively homogeneously on the nanoscale in the PU matrix.

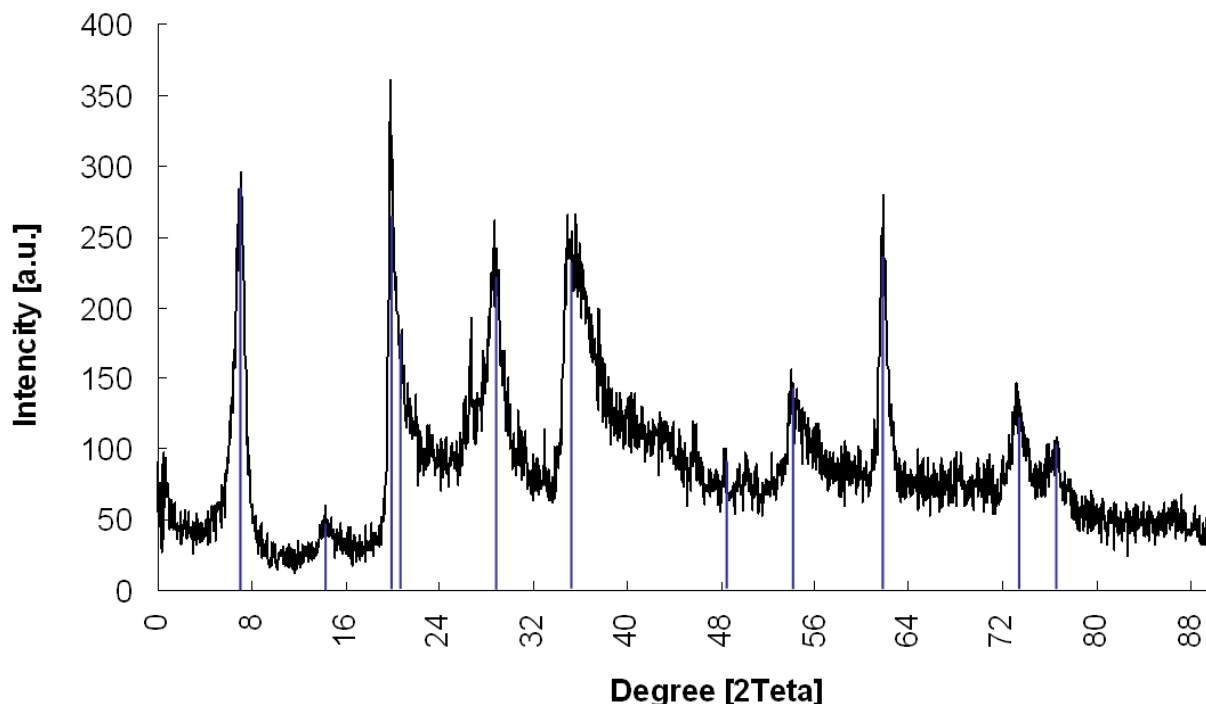


Figure 2. (a) The X-ray diffraction (XRD) pattern of (a) pure polyurethane (PU), (b) pure clay (MMT) and (c) PU/MMT. The numbers in parenthesis give the Miller indices of pure nanoclay (JCPDS19-0629) assigned to the observed peaks.

4.3. TEM

To obtain more accurate information on the morphology of the nanoclay TEM measurements were made. These showed that the MMT keeps its layered pattern inside the composite indicating that the PU penetrate through the MMT layers resulting in an intercalated structure. Pure clay and PU/MMT the result for which are shown in Fig. 4 exhibits a particle reinforced composite structure and in this case the particle surface area could be determined directly using the image analysis technique. In this technique areas within a microscopic image are identified through their contract area and edge intensity level. It is normally restricted to subconfluent systems and consequently the visible projected nanoparticle area (A) is only an indicator of the actual area of contact between particle and matrix. Fig. 5 shows a bar chart of equivalent diameter calculated as $\sqrt{\frac{4A}{\pi}}$ of the nano size distribution.

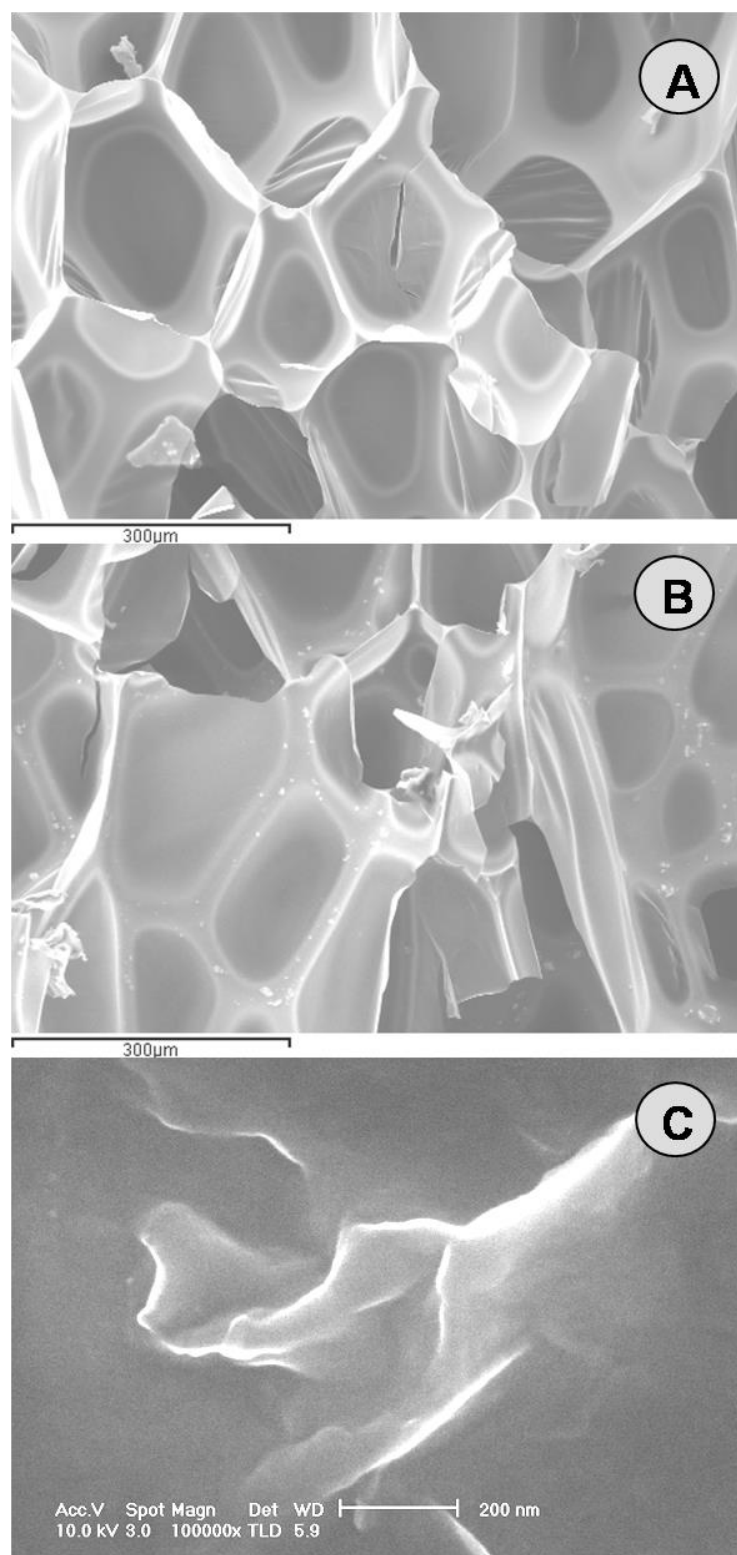


Figure 3. SEM photographs of: (a) pure PU; (b) PU/MMT; (c) pure nanoclay.

4.4. Morphology vs. mechanical Structure

The impact response of the nanocomposite with 2.5 and 10 wt. % MMT were evaluated. Several samples of each set were tested at different energy levels. Transient data including time, load, energy, velocity and deflection were collected for each sample as functions of time. Fig. 6 compares typical load versus time curves for the two specimen types at 19.5 J impact energy level. The peak loads were 70.64 kN for 2.5 wt. % MMT loaded composites and 72.84 kN for the wt. % MMT loaded sample.

Under impact loading, energy absorption in any material is mainly through elastic deformation in the initial stage with some energy absorbed through friction. Once the materials yield stress, the level of maximum elastic deformation, is reached the structure starts deforming irreversibly. The structure then dissipates the excess energy in the form of either plastic deformation in case of ductile materials or through various damage mechanisms in the case of brittle materials. It was further noted that samples with higher filling percentage had the highest energy intake at the failure point, in agreement with previous observations by Njuguna [11].

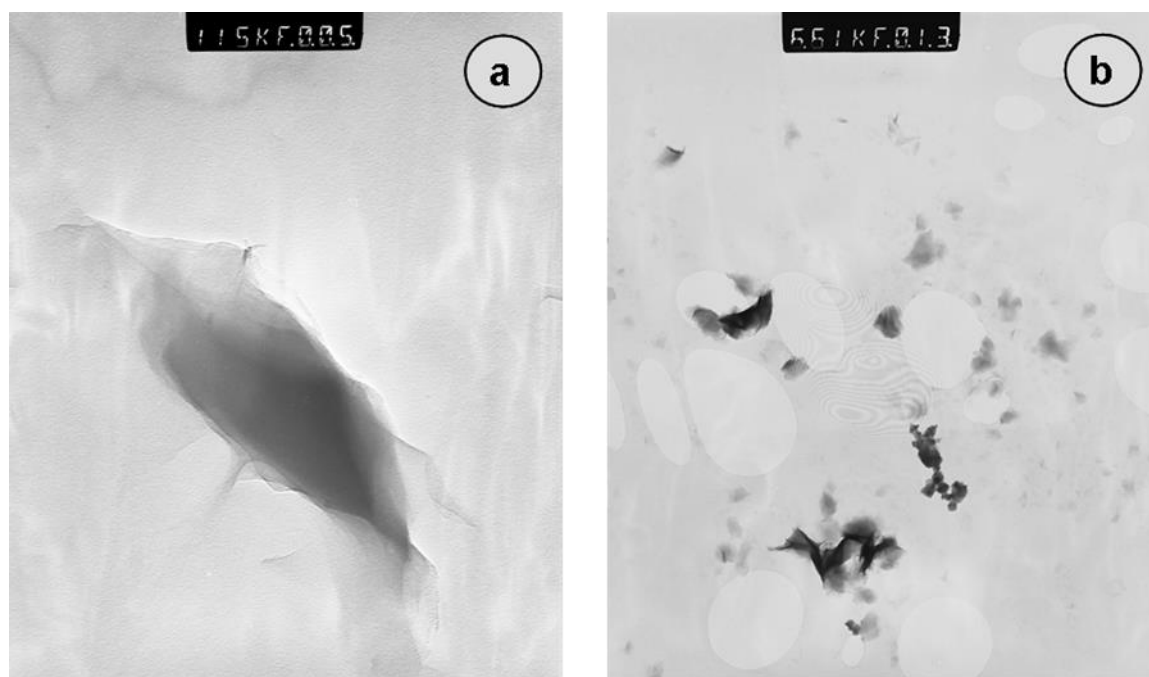


Figure 4. TEM microphotograph of: (a) pure nanoclay; (b) PU/MMT.

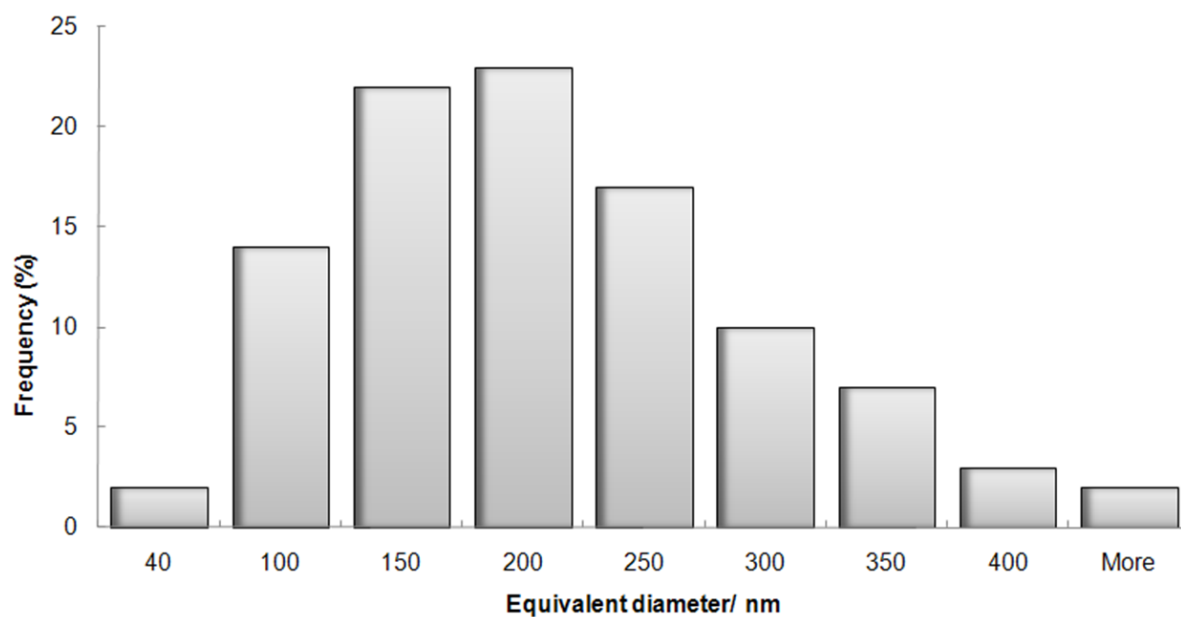


Figure 5. Bar chart of the equivalent diameter of MMT layers from a typical preparation determined from TEM images (a total of 100 particles were measured).

5. Conclusion

Fabricated PU/MMT nanocomposites have been subjected to XRD, SEM and TEM analyses and these show that the clay has the correct crystalline form and still retains a good dispersion of nanoparticles in the PU matrix. SEM examination of a clay/waterborne polyurethane nanocomposite showed that the clay was distributed in the region in which hard segment aggregation of polyurethane was located.

As demonstrated in a previous study [11] the incorporation of MMT increases the number of PU cells with smaller dimensions and higher anisotropy index. The reduction of pore size increased the composite density, so that composites with increasing amount of nanofiller were able to taking higher peak loads. Under impact loading, energy absorption in any material is mainly through elastic deformation in the initial stage with some energy absorbed through friction [20,21]. Once reached the materials yield stress, the level of maximum elastic deformation is reached the structure starts deforming irreversibly. The structure then dissipates the excess energy in the form of either plastic deformation in the case of ductile materials or through various damage mechanisms in the case of brittle materials. It was further noted that samples with higher filling percentage had the highest energy intake at failure point, in agreement with previous observations in the literature.

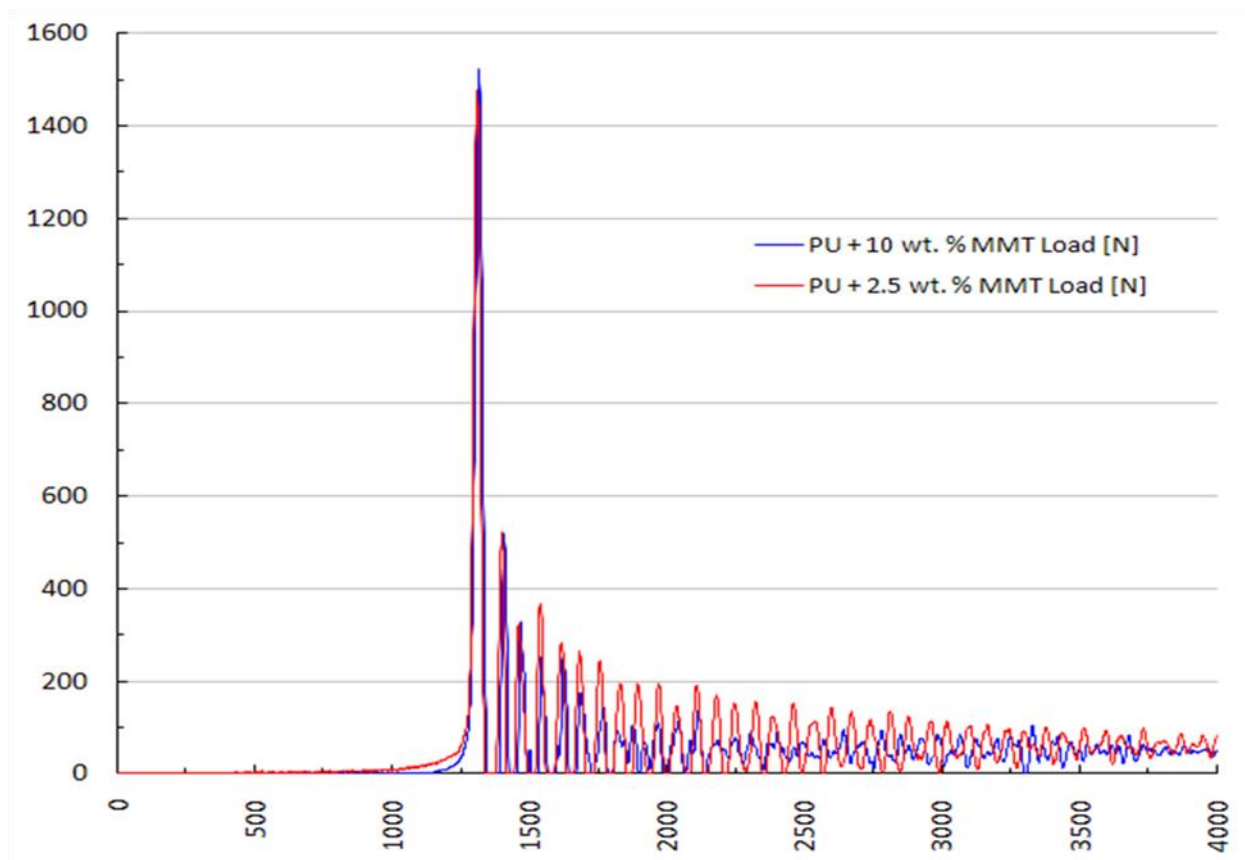


Figure 6. Comparison of load vs time for the two specimen types at 19.5 J impact energy level. The peak loads were 70.64 kN for 2.5 wt. % MMT loaded composites and 72.84 kN for the wt. % MMT loaded sample.

6. References

- [1] L.P. Cheng, D.J. Lin, K.C. Yang, *J. Membr. Sci.* 2000, 172, 157-166.
- [2] G. Jimenez, N. Ogata, H. Kawai, T. Ogihara, *J. Appl. Polym. Sci.* 1997, 64 (11), 2211-2215.
- [3] E.P. Giannelis, *Adv. Mater.* 1996, 8, 29-35.
- [4] P.C. LeBaron, Z. Wang, T.J. Pinnavaia, *Appl. Clay Sci.* 1999, 15, 11-29.
- [5] M. Alexandre, P. Dubois, *Mater. Sci. Eng.* 2000, 28: 1-65.
- [6] K.J. Yao, M. Song, D.J. Hourston, D.Z. Luo, *Polym.* 2002, 43 (3), 1017-1020.
- [7] T.K. Chen, Y.I. Tien, K.H. Wei, *J. Polym. Sci., Part A: Polym. Chem.*, 1999, 37, 2225-2233.
- [8] Q. Wu, Z. Xue, Z. Qi, F. Wang, *Polym.* 2000, 41, 2029-2032.
- [9] H. Dvorchak, *J. Coatings Technology*, 1997, 69, 47-52
- [10] C. Hongxiang, Z. Maosheng, S. Hongying, J. Qingming, *Mater. Sci. Eng.* 2007, 725-730.
- [11] J. Njuguna, K. Pielichowski, S. Desai, *Polym. for App. Technologies* 2008, 19(8), 947-959.
- [12] L. Tie, J.P. Thomas, *Chem. Mater.* 1994, 6, 2216-2219.
- [13] K. Masaya, *J. Polym. Sci. Part A: Polym. Chem.*, 2004, 42, 819-824.
- [14] A. Okada, A. Usuki, *Mater. Sci. Eng.* 1995, C3: 109-115.
- [15] M. Alexandre, P. Dubois, *Mater. Sci. Eng.* 2000, 28, 1-63.

- [16] M. Kurian, A. Dasgupta, M.E. Galvin, C.R. Ziegler, F.L.Beyer, *Macromolecules*, 2006, 39, 1864-1871.
- [17] *Nanoscience and Nanotechnologies*, The Royal Society & the Royal Academy of Engineering, July 2004, (Reproduced in part with permission 2005).
- [18] RTO Lecture Series, Nanotechnology aerospace applications. EN-AVT-129, May 2005.
- [19] G. Chen, Y. Ma, Z. Qi, *Scripta Mater.* 2001, 44, 125-128.
- [20]. J. Njuguna, S. Michalowski, K. Pielichowski, K. Kayvantash, A. C. Walton, 2010, *Polymer Composites*, 2010: 32(1), 6–13.
- [21] L. Sun, R. F. Gibson, F. Gordaninejad, J. Suhr, 2009, 69, 2392-2409.